

Radio-frequency size effect in impurity diffusion

S. V. Gudzenko

Institute of Physics Problems, USSR Academy of Sciences

I. P. Krylov

Crystallography Institute, USSR Academy of Sciences

(Submitted 29 December 1983)

Zh. Eksp. Teor. Fiz. **86**, 2304–2315 (June 1984)

We investigate experimentally and theoretically a new type of radio-frequency size effect (RSE) due to cutoff of the electron trajectories in a layer of impurity atoms that have diffused into the interior of a single-crystal metal. A method is developed for calculating the position and shape of the RSE line from the signal in the initial sample. Comparison of the experimentally observed and calculated RSE lines yields the impurity diffusion coefficient, accurate to 3%. The proposed new method of measuring the diffusion coefficient has higher accuracy and sensitivity than the known methods, and the measurements and data-reduction procedures are simpler. The coefficients of diffusion of four metals in indium single crystals were measured and the activation energies determined.

Measurement of the surface impedance of pure metals as a function of the magnetic field reveals the contribution made to the surface currents by the electrons returning to the skin layer after moving on orbits in the interior of the metal to distances of the order of their mean free path l . Modern technology is capable of producing metal single crystals with l on the order of several millimeters and more. Under these conditions measurement of the impedance can yield information on the processes that take place in the metal at considerable distance from a surface irradiated at radio frequencies. In the case of plates of thickness $d \lesssim l$ the interaction of the electrons with the opposite face of the sample produces the many radio-frequency size effects (RSE) that were investigated earlier (see, e.g., the review by Kaner and Gantmakher¹).

Obviously, however, this method can be used in principle also to study the interaction of the electrons with any inhomogeneity of the metal structure. We have already published² a preliminary report of an observed RSE of a new type, produced when electrons diffuse in a layer of impurities that had diffused into a sample. We describe below the results of a more detailed investigation of this effect. It is of interest in view of the possibility of using an RSE procedure to study the diffusion of low-density impurities in a pure-metal single crystals.³ In observation of the RSE in a plane-parallel plate one measures the surface impedance $Z = R + iX$ in a homogeneous constant field $\mathbf{H} \perp \mathbf{n}$, where the vector \mathbf{n} is the normal to the flat surface of the sample. An RSE line of the "cutoff" type is produced in a field $H = H_0$ at which the trajectory of the electrons of the extremal cross section is equal to the sample thickness d , so that the effective electrons accelerated in the skin layer at one surface of the plate are diffusely scattered (cut off) by the opposite surface. If we denote by $2p$ the size of the extremal section of the Fermi surface in the $\mathbf{n} \times \mathbf{H}$ direction, then $H_0 = 2pc/ed$. The RSE linewidth is $(\Delta H/H_0) \sim \delta/d$, where δ is the skin-layer depth.

It was observed in Ref. 2 that if $Z(H)$ is measured for one surface of the sample, and a film of metal that can diffuse

into the plate is deposited on the opposite surface, the RSE line is shifted to fields $H'_0 > H_0$ for all the extremal sections. The value of H'_0 increases with increasing diffusion time t . The impression is gained that the electron trajectories are cut off by an impurity layer of thickness

$$\Delta = d(1 - H_0/H'_0). \quad (1)$$

We shall show presently that although the diffusing impurity layer does not have clear-cut boundary, the probability of scattering of an electron as it penetrates into a dirty-metal layer increases so rapidly that the RSE line shift is $H'_0 - H_0 > \Delta H$, where ΔH is the linewidth. The sample becomes in effect thinner.

EXPERIMENTAL PROCEDURE

The experiments were performed with an indium single crystal of high purity, containing $\sim 10^{-4}\%$ of impurities. The samples, disks 18 mm in diameter and about 0.3 mm thick, had mirror-smooth plane surfaces. They were grown from the melt in a dismountable mold. The mold was an assembly of flat glass plates and steel liners, forming a cavity in which the indium was poured. An organic film and a thin layer of lampblack deposited on all surfaces in contact with the molten indium prevented sticking of the sample to the glass and possible dissolution of steel impurities. By assembling a stack of several glass plates alternating with liners, having a common channel for pouring the indium, we produced in one pouring up to five identical samples. Measurement of the helicon damping⁴ and of the RSE at the limiting point¹ yielded for the electron mean free path of the electrons in our sample an estimate $l \approx 1$ mm.

The impurity-metal films were deposited by evaporation in vacuum on the sample surface, which was cleaned beforehand by vacuum sputtering in high-purity argon. A diagram of the apparatus for the film deposition is shown in Fig. 1. The sample was placed on a copper stand, and protected from overheating by soldering two peripheral points to the stand with a flexible cold finger. A protective glass ring prevented the copper from evaporating during the time

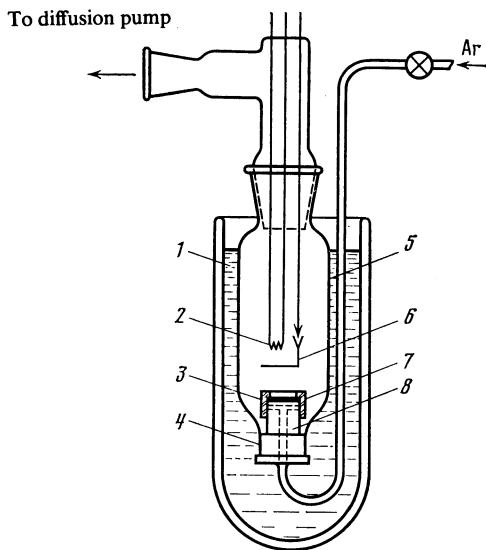


FIG. 1. Diagram of apparatus for depositing metal films: 1—liquid nitrogen, 2—evaporator, 3—guard ring, 4—glass-to-metal junction, 5—glass bulb, 6—shutter serving as anode, 7—sample, 8—copper stand.

of action of the glow discharge. The discharge was produced at a pressure $\approx 5 \times 10^{-2}$ Torr, with the argon passing through the gap between the guard ring and the lateral surface of the stand and flowing over the upper surface of the sample. An indication of successful cleaning of the sample surface was the appearance of a shiny indium layer on the inner cylindrical surface of the guard ring. After stopping the argon flow, a high vacuum, $\sim 10^{-5}$ Torr, was produced

within one minute and evaporation of the impurity metal began. After evaporation of the contaminated surface the impurity charge, the aluminum shutter, which served as the anode, was set to rotate and an impurity film several microns thick was deposited on the indium single crystal. During the film-deposition time the sample temperature was close to 100 K. This was verified in control experiments by a thermocouple soldered to the sample.

The impedance was measured with an autodyne oscillator with an inductance coil of shape such that an appreciable part of each turn was a straight line, and these sections of all turns were in a single plane. This planar part of the coil was clamped to the sample surface not coated by the diffusing metal. The coil together with the sample was mounted in a holder that obviated the need for displacing the sample relative to the coil and holder when the measurements in liquid helium alternated with the repeated diffusion annealing.

The diffusion annealing of the samples at above room temperature was carried out in a vapor thermostat in which a constant temperature within not more than 0.5°C was maintained by the vapor of boiling liquid. During the prolonged anneals at room temperature a temperature stability $\pm 0.5^\circ\text{C}$ was ensured by a system that controlled the air temperature in the laboratory. The holder with the sample was immersed in liquid helium during the interval between the diffusion anneal and the measurement of RSE at helium temperatures.

The autodyne oscillator operated in the frequency range $\nu = 2-3$ MHz. The frequency was recorded with standard electronic devices. The constant field was modulated at a frequency 20 Hz and the recorded signal was proportional

TABLE I

Sample No.	Orientation*	$d, \mu\text{m}$	Impurity metal	$T_{\text{anneal}}, ^\circ\text{C}$	$C_0, \text{at } \%$	** $t_{\text{max}}, \text{hr}$
1	[100], 6°	300	Pb	22	12	250
2	»	»	»	120	13	7
3	[100], 1°	340	Pb	22	12	$2 \cdot 10^4$
4	»	»	»	100	13	26
5	»	350	Cd	100	15	30
6	[100], 7°	340	»	100	15	50
7	[100], 1°	330	»	22	5	3000
8	»	335	Bi	100	7	40
9	»	330	Bi	22	4	1500
10	»	330	Al	150	0	5
11	[100], 2°	330	Ag	22	0,0014	6
12	»	»	»	100	»	0,5

Sample No.	$\Delta_{\text{max}}, \mu\text{m}$	$\sigma, 10^{-16} \text{ cm}^2$	$D, \text{cm}^2/\text{sec}$	$\varepsilon_a, \text{eV/at}$	$D_0, \text{cm}^2/\text{sec}$
1	10	1,0	$(6,5 \pm 1) 10^{-14}$	0,82	5,76
2	45	»	$(6,0 \pm 1) 10^{-11}$	»	»
3	90	1,0	$(6,0 \pm 0,5) 10^{-14}$	»	»
4	70	»	$(5,0 \pm 0,5) 10^{-11}$	»	»
5	170	0,58	$(1,5 \pm 0,1) 10^{-10}$	0,75	2,02
6	200	»	$(1,3 \pm 0,03) 10^{-10}$	»	»
7	80	»	$(3,1 \pm 0,1) 10^{-13}$	»	»
8	170	3,00	$(8,5 \pm 0,5) 10^{-11}$	0,60	0,012
9	70	»	$(6,0 \pm 0,5) 10^{-13}$	»	»
10	0	?	—	—	—
11	40	2,20	$(4,5 \pm 0,5) 10^{-10}$	0,51	0,22
12	120	»	$(3,0 \pm 0,5) 10^{-8}$	»	»

*The angle indicated is between the cited crystallographic direction and the normal n.

**The maximum annealing time is indicated.

to the derivative:

$$\frac{\partial v}{\partial H} \approx -\frac{\partial X}{\partial H}.$$

Twelve samples were used for the detailed investigations of the RSE with impurity diffusion. The characteristics of these In single crystals and other experimental conditions are listed in Table I.

DISCUSSION OF RESULTS. PRELIMINARY DETERMINATION OF THE DIFFUSION COEFFICIENT

Figure 2 shows typical plots of the RSE lines shifted to stronger fields with increasing diffusion-anneal time t . Using as the cutoff field H'_0 the starting point of the line on the weak-field side,¹ we calculated from Eq. (1) the effective decrease of the sample thickness Δ . Some of these results are shown in Fig. 3. Within the limits of experimental error, which is caused mainly by the uncertainty of H'_0 , we have $\Delta \propto \sqrt{t}$. To determine the connection between the ratio Δ/\sqrt{t} and the diffusion coefficient D , we introduce the coordinate frame shown in Fig. 4, with x axis perpendicular to the plane of the sample surface. The impurities diffuse from the surface $x = 0$, while the surface $x = d$ is irradiated from the outside by an electromagnetic field.

The solution of the diffusion equation $\partial C/\partial t = D\partial^2 C/\partial x^2$ for an impurity density C at a constant coefficient D is well known (see, e.g., Ref. 5). In the most widely used case when the solubility limit is $C_0 < 1$, the boundary condition at $x = 0$ yields $C(0, t) = C_0$ and the solution of the diffusion equation takes the simple form

$$C(x, t) = C_0 \operatorname{erfc}(x/2\sqrt{Dt}).$$

Here and below we use standard notation for the complementary error function

$$\operatorname{erfc}(\xi) = 1 - \operatorname{erf}(\xi) = \frac{2}{\sqrt{\pi}} \int_{\xi}^{\infty} e^{-\eta^2} d\eta.$$

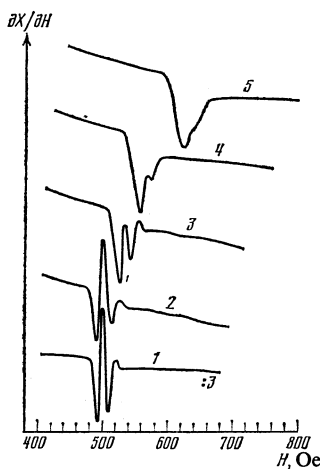


FIG. 2. Plots of RSE lines of sample 8, $\mathbf{H} \parallel [001]$, $\nu = 2.3$ MHz, $T = 1.4$ K. Curve 1 was plotted immediately after casting the sample, and was plotted at an apparatus sensitivity decreased to one-third, curve 2 was plotted after depositing the Bi film and annealing at 22 °C for 1 hr, curves 3, 4, and 5 were plotted after annealing at 100 °C for 0.5, 1.0, and 5.0 hr, respectively.

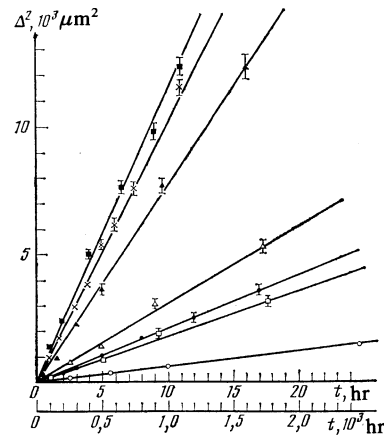


FIG. 3. Shift Δ of RSE lines vs the time t of diffusion annealing. The scale of the upper t axis is for the filled symbols and for the crosses, and the lower is for the light symbols. The symbols correspond to the following samples: 3—○, 4—●, 5—■, 6—×, 7—□, 8—▲, 9—△.

The asymptotic approximation $\operatorname{erfc}(\xi) \approx \pi^{-1/2} \xi^{-1} e^{-\xi^2}$ at $\xi \gg 1$ shows that with increasing argument $\operatorname{erfc}(\xi)$ decreases very rapidly. For example, a ratio $C/C_0 \approx 10^{-3}$ is obtained already at $x = 5\sqrt{Dt}$.

The probability for the passage of an electron through the impurity layer is given by

$$W = \exp\left(-\sigma \int n dr\right),$$

where the integration with respect to the length element dr is along the trajectory, σ is the effective cross section for electron scattering by the impurity atoms, $n = n_0 C(x)$, and n_0 is the density of the atoms of the pure samples (we assume that $C \ll 1$). The electron trajectories that determine the RSE lines investigated by us in the In single crystals are shown in Fig. 4. Exact information on all the details of the trajectory shapes is provided by the results of Refs. 6 and 7. The sec-

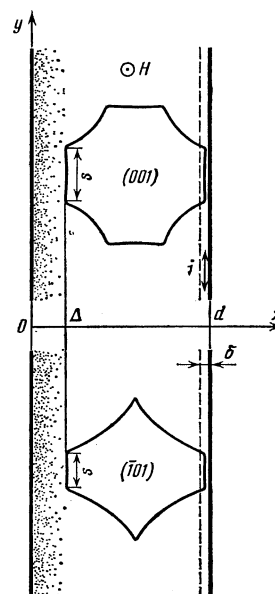


FIG. 4. Projections of extremal electron trajectories in In.

tions tangent to the sample surface do not deviate from linearity by more than 2%. The curvature radii of the rounded junctions between these sections and the remainder of the trajectory amount to less 0.1 of $2p = 2.62 \times 10^{-9}$ g·cm/sec. As a preliminary estimate of D we can thus assume that the electrons negotiate a path s in an impurity layer at one and the same depth $x = x_1$. The equation for the pass-through probability is then

$$W \approx \exp(-A \xi_1^{-1} e^{-\xi_1^2}), \quad (2)$$

where $\xi_1 = x_1/2\sqrt{Dt}$ and $A = \sigma n_0 C_0 s / \sqrt{\pi}$. The quantity σ averaged over all the states on the Fermi surface could be obtained by comparing the data of Ref. 8 on the resistivity ρ of indium with the specified impurity density and with the measured⁹ product ρl for thin cylinders, where l is determined by the sample diameter. The values of σ are listed in the table. The density of the indium atoms was assumed to be $n_0 = 3.83 \times 10^{22}$ cm⁻³. The solubility limits of the various impurities in In, listed in the table, were taken from Refs. 10-12.

By way of example we have taken the case of the diffusion of Cd at 100°C and calculated at $s = d/4$ the value $A = 1.5 \times 10^3$, the function W , and the derivative $W' = dW/d\xi_1$. These functions are shown in Fig. 5. It is clear from this figure that the changes of the probability of electron passage through an impurity layer occur near the value $x_1 = x_m$, which corresponds to the maximum of the derivative W' in the interval $\Delta x_1 \approx \sqrt{Dt}$. Thus, for a preliminary determination of D we can assume that the measured effective decrease of the sample thickness is $\Delta = x_m \approx 5\sqrt{Dt}$. At short diffusion times we have $\sqrt{Dt} < \delta$ and the line shift occurs without a noticeable increase of its width. At long times we get $\sqrt{Dt} > \delta$ and the line shift is accompanied by line broadening, as is actually observed in experiment.

A characteristic feature is that the change of the parameters that determine the coefficient A in (2) has little effect on the ratio x_m/\sqrt{Dt} . Thus, when the coefficient is increased tenfold the derivative W' has a maximum at $x_m/\sqrt{Dt} \approx 6$. This allows us to estimate D without knowing the exact value of σ or C_0 . For estimates, the form of the trajectory is also immaterial. For example, for circular trajectories of radius

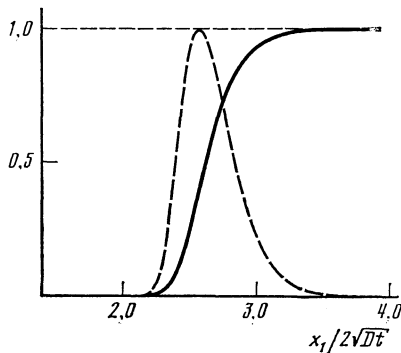


FIG. 5. Plot of the function $W = \exp(-1.5 \times 10^3 \xi_1^{-1} e^{-\xi_1^2})$ (solid curve) and of the derivative, referred to its maximum value 0.53 ($dW/d\xi_1$) (dashed).

R we obtain at $\xi_1 \ll 1$ the formula

$$W \approx \exp(-B \xi_1^{-1/2} e^{-\xi_1^2}), \quad (3)$$

where $B = \sigma n_0 C_0 (2R \sqrt{Dt})^{1/2}$. At typical values of the parameters, expression (3) describes approximately the same function as plotted in Fig. 5.

The values of D obtained from the shifts of the RSE lines by the method described above served as an initial approximation for the recalculation method described in the next section. The difference between the approximate and exact values ranged from 20 to 50%, depending on the relations between the different parameters.

CALCULATION OF THE LOCATION AND SHAPE OF THE RSE IN THE CASE OF IMPURITY DIFFUSION

The density j of the radiofrequency currents is given by

$$j = j_v = \frac{2e}{(2\pi\hbar)^3} \int v_v f d^3p, \quad (4)$$

where the universal constants e and \hbar have the usual meaning, $f = f(x, p)$ is the nonequilibrium increment to the equilibrium electron distribution function $f_0(\epsilon)$, and ϵ , p , and v are respectively the energy, momentum, and velocity of the electrons.

The function f can be obtained by solving the kinetic equation. Its solution takes, in the approximation linear in the electric field $E(x, t)$, the form (see, e.g., Ref. 1)

$$f(\mathbf{r}, \mathbf{p}) = e \frac{\partial f_0}{\partial \epsilon} \int_{r_0}^{\mathbf{r}} \exp\left[-\int_{r_1}^{\mathbf{r}} \frac{|d\mathbf{r}_2|}{l(\mathbf{r}_2)}\right] \mathbf{E}(\mathbf{r}_1) d\mathbf{r}_1. \quad (5)$$

Both integrals are taken here along the trajectory of an electron that arrived at the point \mathbf{r} in the state \mathbf{p} . The inner integral takes into account the distribution-function relaxation in terms of the mean free path $l = l(\mathbf{r})$, which depends on the coordinate by virtue of the inhomogeneous distribution of the electrons. The lower integration limit \mathbf{r}_0 of the outer electron is the starting point, at which the distribution function was at equilibrium. For trajectories that start out on the sample surface with the diffuse electron scattering, \mathbf{r}_0 has a definite finite value. In all other cases \mathbf{r}_0 stands for an infinitely remote point or, in the case of closed trajectories, for a point separated from the end point \mathbf{r} by a large number of revolutions.

To simplify the reasoning, we make two assumptions. First, we neglect the contribution to the integral (5) from those trajectories whose initial point \mathbf{r}_1 is separated from \mathbf{r} by two or more revolutions. This approximation is justified because in our experiments $\pi d/l \approx 1$. Second, we neglect the spikes of the alternating fields and currents in the interior of the metal. We shall assume that the alternating field differs from zero only in the skin layer.

Consider the contribution made to the current \tilde{j} by trajectories that produce an RSE line in an initial sample without diffusing impurities. The integral of (5) used to calculate \tilde{j} is evaluated along trajectories that pass once through the skin layer, while the integral (4) is calculated over the states for sections close to the extremal ones. The contribution of the remaining trajectories near $H = H_0$ depends little on the field and the RSE signal is

$$\left(\frac{\partial X}{\partial H}\right)_{H \gg H_0} \approx \frac{\partial}{\partial H} \left(\int_0^d j(x) dx \right) \approx \frac{\partial}{\partial H} \left(\int_0^d \tilde{j}(x) dx \right). \quad (6)$$

The function $\tilde{j}(x)$ is connected in a simple manner with the observed RSE line shape in the case of extremal sections, for which the dimension of the trajectory is determined by the distance between straight-line sections parallel to the sample surface; on all the remaining trajectory sections the electrons move at a certain angle to the sample surface. For such a Fermi-surface model it can be assumed in the case of diffuse scattering of the electrons by the metal surface that

$$\tilde{j}(x) = \tilde{j}_\infty(x) \theta(x - 2pc/eH),$$

where $\tilde{j}_\infty(x)$ is the density of the currents in an unbounded sample and depends little on H , while $\theta(\xi)$ is a step function with $\theta(\xi) = 1$ at $\xi > 0$ and $\theta(\xi) = 0$ at $\xi \leq 0$. The derivative $\partial\theta/\partial\xi = \delta(\xi)$ is a delta function. Equation (6) takes then the form

$$\left(\frac{\partial X(H)}{\partial H}\right)_{H \gg H_0} \approx \int_0^d \frac{\partial \tilde{j}(x, H)}{\partial H} dx = \int_0^d \tilde{j}_\infty(x) \delta\left(x - \frac{2pc}{eH}\right) dx = \tilde{j}_\infty\left(\frac{2pc}{eH}\right). \quad (7)$$

We consider now RSE in indium plates with diffusing impurities. We isolate the electron-scattering processes due to the inhomogeneous distribution $C = C(x)$ of the diffusing impurities, so that $1/l = 1/l_b + n_0 C \sigma$, where the quantity l_b that does not depend on the coordinates is determined by the phonons and residual impurities in the initial sample.

For trajectories that determine the RSE, we rewrite Eq. (5) in the form

$$\tilde{j}(\mathbf{r}, \mathbf{p}) = e \frac{\partial f_0}{\partial \epsilon} \left\{ \int_{r_0}^{\mathbf{r}} \exp\left[-\frac{L(\mathbf{r}_1, \mathbf{r})}{l}\right] \mathbf{E}(\mathbf{r}_1) d\mathbf{r}_1 \right\} \times \exp\left(-n_0 \sigma \int_{r_0}^{\mathbf{r}} C |d\mathbf{r}_2|\right). \quad (8)$$

The integral

$$J_1 = \int_{r_0}^{\mathbf{r}} C |d\mathbf{r}_2|,$$

over that section of the trajectory which passes in the "dirty" metal layer can be isolated because at these points we assume that $E(\mathbf{r}_1) = 0$. For trajectories of a definite size and shape, the probability

$$W = \exp(-n_0 \sigma J_1) = W(x_1)$$

of going through a layer of dirty metal is a function of only the coordinate x_1 , the minimum distance to the surface $x = 0$. In our simplified reasoning we assume that the trajectories of the sections close to the external ones have the same shape and close dimensions. This assumption allows us to take the factor W out of the integral over the states when j is calculated by Eq. (4). Noting that the factor in the curly brackets of (8) yields after integration over the state an increment to the current density $\tilde{j}_\infty(x)$ in the initial sample without the diffusing impurities, we can write for the increment to the current density in the skin layer in the presence of a

diffusion front

$$\tilde{j}(x) = \tilde{j}_\infty(x) W(x_1) \quad \text{at } x_1 = x - 2pc/eH. \quad (9)$$

We have substituted in (9) the current density for an infinite sample, so that cutoff at $x = 0$ cannot manifest itself because of a sufficiently dense impurity layer; in other words, for a trajectory tangent to the surface $x = 0$ the value of W is practically zero.

Expression (9) is our sought end result. We cannot calculate the RSE line shape from "first principles." Expression (9), however, can yield the signal that can be expected in a sample with diffusing impurities if we know the "initial" $(\partial X/\partial H)_0$ line on a sample without a deposited film. Using (7) and (9) we obtain for the RSE line in a plate with a diffuse layer of impurities

$$\frac{\partial X(H)}{\partial H} \approx \int_{H_0}^{\infty} \left(\frac{\partial X(H_1)}{\partial H_1}\right)_0 W' \left(\frac{2pc}{eH} - \frac{2pc}{eH_1}\right) dH_1, \quad (10)$$

where $W'(x_1)$ stands for t derivative $dW(x_1)/dx_1$ taken at the point x_1 .

In the derivation of (10) we have assumed that the initial line is formed on account of purely diffuse scattering. It is known at the same time that after the melting a noticeable fraction of the electrons can be reflected specularly from the sample boundary. We have therefore assumed it to be more correct to choose as the initial lines an RSE plot obtained immediately after depositing the impurity film (see, e.g., curve 2 of Fig. 2). In our procedure, after sputtering the film, the sample was heated to room temperature and mounted in the helium-apparatus holder for 10 minutes. During that time the impurities diffused to a depth $\sim 10^{-4}$ cm. This was not accompanied by a noticeable line shift, but the shape changed somewhat and the amplitude decreased by several times. We note also that after sputtering the film, as follows

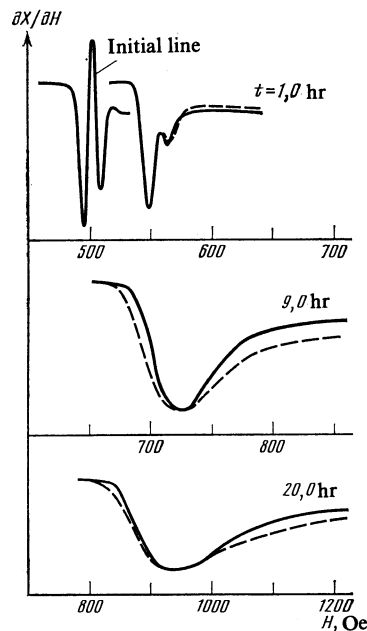


FIG. 6. Comparison of the experimental RSE lines (solid) and those recalculated in accordance with Eq. (10) (dashed) for sample No. 6.

from an analysis of the extrema, the RSE line widths increased by 10–15%. It is of interest to note that in experiments with samples whose surfaces were subjected to cathode sputtering without depositing a film, the described changes of the RSE line were weaker by several times. This indicates that cathode sputtering does not guarantee fully a diffuse scattering of the electrons.

The RSE lines calculated with the aid of (10) from the initial lines were compared with the experimental curves. An example of such a comparison is shown in Fig. 6 for the case $\mathbf{n}||[101]$. In the calculation of the path integral that determines W we took into account the deviation from linearity of the trajectory section s . For the rounding radius that connects this section with the rest of the trajectory we assumed a value $R = s/3$. We thus obtained the following approximation, which was used in the calculations:

$$W(x_1) = \exp \{ -\sigma n_0 C_0 [0, 2s \operatorname{erfc}(\xi_1) + 0, 8s \operatorname{erfc}(\xi_2) + \sqrt{Dt} F(x_1)] \},$$

where

$$\begin{aligned} x_1 &= (2pc/eH_1 - 2pc/eH), & \xi_1 &= x_1/2\sqrt{Dt}, \\ x_2 &= (2pc/eH_1 - 1, 96pc/eH), & \xi_2 &= x_2/2\sqrt{Dt}, \\ F(x_1) &= 8\pi^{-1/2} Dt x_1^{-2} (1 + x_1 R/Dt)^{1/2} \\ &\quad \times \exp(-x_1^2/4Dt). \end{aligned}$$

The amplitude of the RSE signal after the diffusion anneals turned out to be 1.5–3 times larger than the calculated one. We attribute this to a decrease of the scattering by the annealed defects in the bulk of the sample and to a decrease of the trajectory length in proportion to $1/H'_0$. To compare the location and shape of the line we introduced in (10), after the next anneal, an empirically chosen factor that reconciles the calculated and observed signal amplitudes.

If a correct account is taken of all the factors that determine $W(x_1)$, the error of D is due to the error δH_0 in the measurement of the position of the line, in accord with the relation

$$\delta D/D \approx 2\delta H_0/(H'_0 - H_0).$$

At long times t the RSE line width ΔH increases in proportion to \sqrt{Dt} , as does also the shift $(H'_0 - H_0)$ of the line position. The ratio $\delta H_0/(H'_0 - H_0)$ can only increase as a result of a decrease of the signal/noise ratio. At short times t , on the contrary, the line width ΔH does not depend on \sqrt{Dt} , so that $\delta H_0/(H'_0 - H_0) \sim 1/\sqrt{Dt}$. Thus, the optimal for the most accurate measurement of D is the value of t at which $2\sqrt{Dt} \approx \delta$ (where δ is the thickness of the skin layer). In our experiments, when annealing at temperatures 100 °C, this condition was satisfied for $t = 2-4$ hr. At the optimum value of t the error in the measurement of the line position was usually $\delta H_0 \approx 20$ Oe, and the line shift was $(H'_0 - H_0) \approx 100-200$ Oe, so that a typical error value is $\delta D/D \approx 2-5\%$.

For sample 6, the exact value of the diffusion coefficient, listed in the table, was chosen to equate to positions of the minima of the calculated and observed RSE lines for a diffusion-anneal time $t = 2$ hr. It can be seen from Fig. 6 that the positions of the minima agree with these values also at all

the other values of t . A similar procedure of choosing the diffusion coefficient such that the positions of the experimentally observed line and that calculated from (10) for the optimal annealing time agreed was used also in the other cases. The values of D obtained in this manner are listed in the table. We note that in a number of cases the calculated line shape agreed only approximately with experiment. The error of D was then larger.

Worthy of special notice is the case of the orientations $\mathbf{n}||[100]$ and $\mathbf{H}||[100]$. In this case the RSE line is determined by helical trajectories and depends strongly on the inclination of the vector \mathbf{H} to the sample surface: at a 0.5° inclination the RSE signal reverses sign. Under this condition the RSE signal in exactly the parallel direction also reverses sign during the intermediate diffusion stages, when $\sqrt{Dt} \approx \delta$. We could not find a satisfactory explanation of this phenomenon. This question, as well as the change of the line shape upon inclination of the field \mathbf{H} , remains open.

A few remarks concerning the obtained values of D . These coefficients were unknown for the diffusion of all the investigated impurities in In, except Ag. In the case of Ag diffusion, our data agree with those of Ref. 13. The diffusion of Ag impurities has a number of distinguishing features. In contrast to the Pb, Cd, and Bi impurities, which for substitutional solutions and their displacement in the In matrix requires the presence of vacancies in the neighboring sites, the Ag atoms diffuse through the interstices.¹³ In view of the mechanism of Ag diffusion, the coefficient D turned out to be two decades larger than in the remaining cases. At the same time, the solubility C_0 for Ag is very small, so that the factor A in (2) turns out to be of the order of unity. This causes a strong broadening of the RSE line in the case of Ag diffusion.

The experiments with Al impurities are an isolated case. The RSE line did not shift noticeably after sputtering the Al film and annealing for many hours at a temperature close to the melting point of In. According to the conclusion of Ref. 8, Al apparently does not dissolve in In.

By comparing the data at two temperatures with the thermally-activated-diffusion formula $D = D_0 \exp(-\varepsilon_a/kT)$ we determined the activation energy ε_a and the pre-exponential factor D_0 . These values are listed in the last two columns of Table I.

ELECTRON REFLECTION FROM A SUPERCONDUCTING FILM

Coating a superconducting metal on the surface of a single crystal can give rise to a superconducting layer with a high critical field H_c exceeding that of pure In. Among the impurities employed, this property was possessed by Pb and Bi. If the interface of the normal and superconducting phases lies at a depth x_s such that the function $W(x_s)$ is not very small, the electrons have a noticeable probability of undergoing Andreev reflection. Accordingly, as shown in Ref. 14, a line in a field $H_0/2$ should appear besides the RSE in the field H_0 . We observed the Andreev line after sputtering Pb (Ref. 2), if the diffusion time at room temperature did not exceed $t_1 = 1$ hr. This means that the region in which the

superconducting-ordering parameter or the energy gap are different for zero extended to a depth $x_s \approx 5\sqrt{Dt_1} \approx 1 \times 10^{-4}$ cm.

As shown in Ref. 15, alloys of indium with lead, at a lead density $C \ll 1$ at. %, have a critical field $H_c \lesssim H_0/2 \approx 250$ Oe. In our experiments this density level was at a depth $x_c = 2\sqrt{Dt_1} \approx 5 \times 10^{-5}$ cm. The comparison of x_c with x_s agrees with a coherence length $\xi_0 = 4 \times 10^{-5}$ cm for pure In. No Andreev line was observed after depositing Bi. It appears that the superconducting gap was suppressed in layers with larger impurity density.

CONCLUSION

We investigated a new method of measuring the coefficient of impurity diffusion in single crystals of pure metals, based on the use of the radio-frequency size effect. We succeeded in demonstrating theoretically and experimentally that the scattering of electrons in a layer of atoms that have diffused into the interior of the single crystal can lead to the appearance of a radio-frequency size effect of the cutoff type. Measurement of the magnetic field at which the impedance singularity is observed yields the depth to which the impurity atoms have diffused, and by the same token gives the diffusion coefficient. This method was used to measure the values of D in In single crystals of In for four impurity metals.

The method proposed for measuring the diffusion coefficient constitutes a qualitatively new stage of the research into diffusion processes in metals. The use of single crystals of very pure metals, which are needed for the observation of the radio-frequency size effect, excludes the influence of extraneous impurities and of intercrystalline boundaries on the investigated diffusion process.

The new method ensures high-accuracy measurements of the diffusion coefficient. If the effective cross section for the scattering of the conduction electrons by the atoms of the diffused substance can be calculated theoretically or determined by supplementary experiments, the accuracy with which the diffusion coefficient is measured is limited by the accuracy of the measurement of the magnetic field in which the radio-frequency size effect is observed, and amounts in practice to about 3%. This circumstance makes this method superior to other research procedures in which only the order of magnitude of the diffusion coefficient is estimated. The new method has high sensitivity and can be used to measure very low values of the diffusion coefficient. The radio-frequency size effect line shape can change when the diffused substance penetrates into the single crystal to very small depths, comparable with an interatomic distance $\sim 10^{-7}$ cm. If diffusion to a considerable depth is required, however,

then in our method, in contrast to the method of radioactive isotopes, the duration of the diffusion is in principle not limited. This makes possible measurements of arbitrarily small values of the diffusion coefficient by increasing the duration of the diffusion.

In contrast to all other known methods of determining the diffusion coefficient, the proposed method imposes no limitation whatever on the diffusing substance. Since conduction electrons are scattered by practically any impurity, the radio-frequency size effect permits the study of diffusion of any substance in a single crystal of a pure metal.

In most heretofore known methods of diffusion research it was in principle impossible or very difficult to carry out the investigations at low temperature. The method proposed, in which the need for performing the measurements at low temperatures down to that of liquid helium is connected with the procedure for recording the diffusing atoms, uncovers qualitatively new possibilities of investigating low-temperature diffusion, particularly the diffusion singularities connected with quantum laws and observable only near absolute zero.

The authors are grateful to P. L. Kapitza for the opportunity of performing the study at the Institute of Physics Problems of the USSR Academy of Sciences and to Yu. V. Sharvin for a discussion of the results and for helpful hints.

¹E. A. Kaner and V. F. Gantmakher, Usp. Fiz. Nauk **94**, 193 (1968) [Sov. Phys. Usp. **11**, 81 (1968)].

²S. V. Gudenko and I. P. Krylov, Pis'ma Zh. Eksp. Teor. Fiz. **28**, 243 (1978) [JETP Lett. **28**, 224 (1978)].

³S. V. Gudenko and I. P. Krylov, Inventor's Cert. No. 697883 (USSR). Publ. in Byull. Izobret. No. 42 (1979).

⁴I. P. Krylov, Zh. Eksp. Teor. Fiz. **71**, 1620 (1976) [Sov. Phys. JETP **44**, 848 (1976)].

⁵B. S. Bokshtein, Diffuziya v metallakh (Diffusion in Metals), Metallurziya, 1978, p. 20.

⁶D. B. B. Risenbrij, J. A. Radder, A. B. M. Hoff, and D. G. de Groot, J. Phys. F: Metal Phys. **7**, 2067 (1977).

⁷D. G. de Groot, A. B. M. Hoff, D. B. B. Rijsenbrij, and J. H. P. van Weeren, *ibid.* p. 2077.

⁸B. N. Aleksandrov and V. V. Dukin, Fiz. Nizk. Temp. **2**, 105 (1976) [Sov. J. Low Temp. Phys. **2**, 54 (1976)].

⁹B. N. Aleksandrov, Zh. Eksp. Teor. Fiz. **43**, 399 (1962) [Sov. Phys. JETP **16**, 286 (1963)].

¹⁰A. E. Vol, Stroenie i svoistva dvoynykh metallicheskih sistem (Structure and Properties of Binary Metallic Systems), Fizmatgiz, Vol. I, p. 235, 1959.

¹¹A. E. Vol, *ibid.*, Vol. II, p. 125, 1962.

¹²A. E. Vol and I. K. Kagan, *ibid.*, Vol. III, pp. 321, 428, and 459, 1976.

¹³T. R. Anthony and D. Turbull, Phys. Rev. **151**, 495 (1966).

¹⁴I. P. Krylov and Yu. V. Sharvin, Zh. Eksp. Teor. Fiz. **64**, 946 (1973) [Sov. Phys. JETP **37**, 481 (1973)].

¹⁵R. C. Carriker and C. A. Reynolds, Phys. Rev. B2, 3991 (1970).

Translated by J. G. Adashko